https://doi.org/10.5194/cp-2024-46
Preprint. Discussion started: 4 July 2024
© Author(s) 2024. CC BY 4.0 License.

Climate of the Past Discussions

Stretched polar vortex increases mid-latitude climate variability during the Last Glacial Maximum

Yurui Zhang[1], Hans Renssen[2], Heikki Seppä[3], Zhen Li[1], Xingrui Li[1]

[1] State Key Laboratory of Marine Environmental Science, College of Ocean & Earth Sciences, Xiamen University, Xiamen, China
[2] Department of Natural Sciences and Environmental Health, University of South-Eastern Norway, Bø, Norway
[3] Department of Geosciences and Geography, University of Helsinki, Helsinki, Finland

Correspondence to: Yurui Zhang (yuruizhang@xmu.edu.cn)

Abstract. The Arctic stratospheric polar vortex (PV) is a key driver of winter weather, and has been found playing role in winter climate variability and its predictability in Eurasia and North America on inter-annual and decadal time scales. However, to what extent this relationship also plays a role in driving climate variability on glacial-interglacial time scales is still unknown. Here, by systematically analysing PV changes in four sets of PMIP4 simulations for the last glacial maximum (LGM) and the pre-industrial (PI), we explore how the PV changed during the glacial climate and how it influenced climate variability. Our results show that under LGM conditions, the PV stretched toward the Laurentide ice sheet, which resulted in a less stable ellipse shape that increased the possibility of cold air outbreaks into mid-latitudes. During the LGM, this stretched PV pushed cold Arctic air further equatorward, increasing winter climate variability over the more (southward) southern mid-latitudes. In particular, this strengthened winter cooling over the mid-latitudes beyond the coverage of the Laurentide ice sheet (unlike summer). PV-induced temperature variability also explains the inter-model spread, as removing the PV variation from the model results reduces the inter-model spread by up to 5 ℃ over mid-latitude Eurasia. These results highlight the critical role of PV in connecting the polar region and mid-latitudes on glacial-interglacial time scales. These connections are reminiscent of intra-seasonal stratosphere–troposphere coupling.

Keywords: polar vortex, mid-latitude climate, winter temperature, climate variability, LGM glacial climate

1 Introduction

The stratospheric polar vortex (PV) is an area of high-speed, cyclonically rotating winds in both polar regions. Influenced by atmospheric waves propagated upward from the troposphere, the forming and decaying of PV occur on the seasonal time scale (Baldwin et al., 2003; Kolstad et al., 2010). In the Arctic, it has been found that the PV forms in autumn when Arctic temperatures cool rapidly (Kolstad et al., 2010). The increased temperature difference between the polar region and the

https://doi.org/10.5194/cp-2024-46
Preprint. Discussion started: 4 July 2024
© Author(s) 2024. CC BY 4.0 License.

Climate of the Past Discussions

tropics causes strong winds to develop, and the Coriolis effect causes the vortex to spin up (Baldwin et al., 2003; Baldwin and Thompson, 2009). This PV strengthens when the latitudinal temperature gradient enhances and reaches its maximum in winter. The stratospheric polar vortex breaks down again in spring as the polar region warms up and the latitudinal temperature gradient decreases. These changes in the stratospheric PV strength can feed back to affect weather and climate closer to the Earth surface by adjusting on Arctic air intrusion into mid-latitudes(Baldwin and Dunkerton, 2001; Baldwin et al., 2003). When the stratospheric vortex of the Arctic is strong, there is a single vortex with a jet stream that is well constrained near the polar front, and the Arctic air is well contained. When this northern stratospheric vortex weakens, it breaks into two or more smaller vortices, the flow of Arctic air becomes more disorganized, and masses of Arctic air can push equatorward. These seasonal dynamic changes make PV a main driver for winter weather over mid-latitudes (Kolstad et al., 2010).

Apart from its seasonal change, the Arctic PV is also characterized by considerable inter-seasonal and inter-annual variability (Manzini et al., 2012; Reichler et al., 2012). Influenced by the variation of atmospheric waves from the below troposphere, the stratosphere organizes the chaotic wave forcing and creates long-lived changes (a week to several months) in the hemispheric-scale circulation (McIntyre and Palmer, 1983). This could trigger occasional breaking of stratospheric waves, analogous to ocean waves breaking on a beach, that causes stratospheric air flow becoming more disorganized, and masses of cold Arctic air can push further south, bringing with them a sharp temperature drop (Baldwin et al., 2003; McIntyre and Palmer, 1983). These sporadic occurrences of a weak Arctic PV event have significant impacts on surface weather and climate variability in inter-seasonal and inter-annual time scales (Cai et al., 2024; Kolstad et al., 2010; Manzini et al., 2012). The negative phase of North the Atlantic Oscillation (NAO, defined as the surface sea-level pressure difference between the Subtropical High and the Subpolar Low) in the troposphere is found following the weakening and warming of the stratospheric polar vortex (Yang et al., 2016). In this sense, the Arctic PV variation has been thought as an important driver of weather predictability and the climate variability on inter-annual and decadal time scale over Eurasia and North America (Kim et al., 2014; Kim et al., 2022; Zhang et al., 2022). However, if it also plays a role in climate variability on longer timescale, such as in glacial-interglacial cycle scale, has not been explored yet.

The last glacial maximum (LGM; ~ 21 thousand years ago) is the most recent global cold extreme and has been widely documented by various proxy records (Cleator et al., 2020). The LGM world was very different from the present, with ice sheets covering northern North America and Fennoscandia, in addition to the Greenland and Antarctic ice sheets that are still present today (Clark and Mix, 2002; Peltier et al., 2015). These extensive ice sheets represented large changes in topography and modified the spatial pattern of surface temperatures (Harrison et al., 2015; Kageyama et al., 2021). This alteration is expected to generate planetary waves that can propagate into the stratosphere and affect PV variation, through the active interaction between troposphere and stratosphere (Baldwin et al., 2003; Baldwin and Thompson, 2009).

As for the climate of LGM, many studies, from proxy record compilations to the Paleoclimate Modelling Intercomparison Project (PMIP), and to the data-assimilation, have been carried out to investigate the spatial patterns of the cold climate

https://doi.org/10.5194/cp-2024-46
Preprint. Discussion started: 4 July 2024
© Author(s) 2024. CC BY 4.0 License.

Climate of the Past Discussions

features and their driving mechanisms (Annan et al., 2022; Cleator et al., 2020; Harrison et al., 2015; Kageyama et al., 2021; Tierney et al., 2020). The enhanced cooling at high-latitudes and increased land-sea temperature contrast have been identified as features of glacial climate, as the result of polar amplification (Kageyama et al., 2021). Another common feature emerging from proxy data and PMIP model results is the enhanced winter cooling over mid-latitudes. Proxy-based reconstructions show a 5–8 ℃ more temperature reduction in winter than in summer (Cleator et al., 2020). Model results from PMIP4 and data-assimilation results also reveal enhanced cooling in winter relative to summer (Annan et al., 2022; Kageyama et al., 2021; Tierney et al., 2020). The detailed structure of this enhanced winter cooling at mid-latitudes, however, has large spatial variation and varies widely among models (Annan et al., 2022; Kageyama et al., 2021; Tierney et al., 2020). For instance, two groups presenting data assimilation results give different LGM cooling with zonal profile differences of 3℃ over the mid and high latitudes (Annan et al., 2022; Tierney et al., 2020). Therefore, the research questions to be answered in this paper are: 1) how the Polar Vortex (PV) varied during the LGM glacial climate; 2) more importantly, how the PV changes contributed to the climate variability during the LGM.

2. Methods

2.1 PMIP4-LGM simulations

Given its representativeness of full glacial conditions, the LGM has been the focus of the Paleoclimate Modelling Intercomparison Project (PMIP) since its inception (Braconnot et al., 2012; Braconnot and Kageyama, 2015; Harrison et al., 2015; Kageyama et al., 2017). Key climate drivers considered in these PMIP simulations include the extensive continental ice sheets, lower atmospheric greenhouse gases concentrations, and changes in orbital parameters (Kageyama et al., 2017). Compared with its precedents, the new PMIP4 experimental protocol also includes some changes in newly added forcings. For instance, PMIP4 allows vegetation and atmospheric dust loadings to change accordingly. Therefore, we focus here on PMIP4 results as these represent the most up-to-date simulations of the LGM climate.

We searched for all available PMIP4-LGM simulations from the Earth System Grid Federation (ESGF) database, and found 5 suitable simulations all together (Table 1). Given our interest in exploring the relationship between mid-latitude winter climate and polar vortices, the geopotential height up to stratosphere and air temperature are the two most important variables. The extra variables, such as sea ice extent and sea surface pressure, can enable us to pinpoint the reasons causing these changes. With those target model output variables, six models offer downloadable data for the LGM and PI period from the ESGF database. Notably, since CESM2-FV2 and CESM2-WACCM-FV2 are from the same model family, we only include CESM2-FV2 because the other version included a module for stratospheric chemistry not included in the other PMIP4 simulations (Zhu et al., 2022). In the end, we thus selected four simulation MIROC-ES2L (hereafter MIROC), AWI-ESM-1-1-LR (AWI-ESM), MPI-ESM1-2-LR (MPI-ESM), and CESM2-FV2 (CESM) for our analysis.

https://doi.org/10.5194/cp-2024-46
Preprint. Discussion started: 4 July 2024
© Author(s) 2024. CC BY 4.0 License.

Climate of the Past Discussions

These four selected simulations run with the corresponding models that belong to a fully coupled earth system model. For the MIROC, the atmosphere module is CCSR-AGCM represented with a resolution of 128 x 64 in latitude and longitude, and with 40 vertical layers reaching a top layer of 3 hPa. The oceanic component is COCO4.9 with nested sea ice, utilizes tripolar coordinates with 360 x 256 grids in latitude and longitude, and 63 vertical levels(Hajima et al., 2020). MPI-ESM represents the atmosphere with the ECHAM6 that has 192 x 96 grids in latitude and longitude, with 47 vertical layers reaching a top layer of 0.01 hPa. The marine module is MPIOM1.63, utilizing a grid of 256 x 220 in latitude and longitude, with 40 vertical layers (Mauritsen et al., 2019). The AWI-ESM comprises the atmospheric component ECHAM6 (same as the MPI-ESM), the ocean-sea ice component FESOM, and the terrestrial carbon model JSBACH. Both the atmospheric and oceanic components have an average resolution of around 250 km and 100 km, respectively(Shi et al., 2020). For the CESM2-FV2, the atmospheric component is CAM6, it operates on 144 x 96 grids in latitude and longitude, with 32 vertical layers reaching 2.25 hPa. The oceanic component is POP2 and nested with sea ice module CICE5.1, features a grid of 320 x 384 in latitude and longitude and 60 vertical layers(Danabasoglu et al., 2020).

All these four simulations have been performed with the greenhouse gases by following the protocol given in Kageyama et al. (2017). According to ice core records, the greenhouse gas (GHG) concentrations during the LGM were overall lower than at present (Bereiter et al., 2015). The considered GHG include CO_2, CH_4 and N_2O, which have been prescribed as 190 ppm, 375 ppb and 200 ppb, respectively. As for the orbital parameters, all the simulations were run with the prescribed eccentricity as 0.018994, inclination as 22.949 ° and perihelion as 114.42 ° (Kageyama et al., 2017). These orbital configurations cause a slight decrease of summer solar radiation at Northern Hemisphere high latitudes and an increase in winter insolation with the total magnitude of 10W/m^2 (Kageyama et al., 2017). More detailed information refers to Kageyama et al. (2017; 2021).

2.2 Polar vortex analysis

To investigate the effect of the stratospheric polar vortex on mid-latitudinal climate, we constructed composites of the climate with weak and strong vortex activity and compare them with the average climate state. The composite procedure is based on the vortex strength index (VSI) defined by Kolstad et al., (2010) as: VSI=$-\sum((Z-\bar{Z})cos\varphi)/\sum cos\varphi$, Z is the geopotential height, $\bar{Z}$ is its climatological mean, φ is the latitude, and the sum was performed on all grid points north of 65◦N. The reason for the minus sign is that the vortex is weak when the pressure is high and vice versa (Kolstad et al., 2010). This VSI is a conventional quantity of measuring the vortex variability and has been validated as a reliable indicator for its variation in both seasonal and inter-annual time scales (Zhang et al., 2022).

The yearly varying VSI time series data were calculated according to winter season (DJF) geopotential height at 20hPa, since the Arctic stratospheric polar vortex shows strong seasonal variations. As shown by monthly changes VSI in Figure S1, the VSI calculated from the PI simulations is much weaker during the summer with negative VSI and stays at a stable level of less than -1000. By contrast, it is strengthened during the winter with the positive VSI, and also shows larger inter-annual

https://doi.org/10.5194/cp-2024-46
Preprint. Discussion started: 4 July 2024
© Author(s) 2024. CC BY 4.0 License.

Climate of the Past Discussions

variability (Fig S1). This seasonal variability of PI simulation is similar to the results of EAR5 re-analysis data, suggesting that models be able to catch these variations. Correspondingly, we selected years of strong and weak PV based on their winter (DJF) VSI index using the one standard deviation (σ). The strong PV years are represented by those VSI larger than σ, while the weak PV years are given by those below σ (indicated as red and green dots in Fig S2). It is worth to notice that MIROC shows much less inter-annual variability than the other models. For the PI simulation, MIROC has the σ of 70, which is only 1/3 of as in other models. Further comparison with ERA5 re-analysis suggest that MIROC seems to underestimate their inter-annual variabilities (Fig S2). Similar to the previous analysis, we composite all the weak and strong PV years to denote the climate state of weak and strong vortex, respectively (Kolstad et al., 2010; Zhang et al., 2022).

3. Results and Discussions

3.1 Arctic polar vortex stretched over ice sheets during the LGM

As represented by troughs of low geopotential height of the stratosphere (e.g. at 20 hPa), the winter polar vortex was sitting over the Arctic in the PI climate. The smallest geopotential height is around 245 gpm, with inter-model ranging from 244 gpm in MIROC to 246 gpm in AWI-ESM. The center of PV slightly shifts toward the Atlantic side due to strong N Atlantic Oscillation (NAO), otherwise, it has a well-defined and nearly circular shape, as revealed by contour lines of geopotential height in Figure 1. This overall pattern fits the ERA5 re-analysis data, as shown by the similar shape of 250 gpm contour. The slightly more extensive PV during the PI climate compared to the more recent climate used for the re-analysis is expected, given that the PI climate was a bit colder than the climate for 1940-2024 used for ERA5. This is consistent with the results of 3 out of 4 models (CESM being the exception) (Fig. 1).

Compared to PI, one significant feature of PV during the LGM is that it was stretched toward the American continent. For instance, the contour line of 250 gpm was stretched toward N American by 4-8 ° latitude. Accordingly, the center of PV shifts toward America. Compared among different models, the different LGM response of PV is consistent with their inter-annual variability (Fig S2). For instance, the relatively small LGM response of PV in MIROC is in line with its smaller inter-annual variability with standard deviation of 50 gpm.

It has been illustrated that polar stratospheric variability is largely dominated by vertically propagating Rossby waves of tropospheric origin (Andrews et al., 1987; Charney and Drazin, 1961). During the LGM, the presence of the Laurentide ice sheet in the troposphere, up to 2-3km height, could generate planetary waves in the troposphere by modifying the topography (McIntyre and Palmer, 1983; Polvani and Waugh, 2004). Therefore, the ice-sheets-related planetary wave changes could affect the PV, which can in turn descend and influence the surface climate.

The stretched PV during the LGM climate seems compatible with other studies on polar vortex variations relevant to the climate states. For instance, previous studies on PV decadal variability have shown that the Arctic polar vortex shifted

https://doi.org/10.5194/cp-2024-46
Preprint. Discussion started: 4 July 2024
© Author(s) 2024. CC BY 4.0 License.

towards the Eurasian continent and away from North America in response to the Arctic warming and sea-ice loss, particularly over the Barents–Kara seas in recent decades (Zhang et al., 2016a). Our study reveals that the PV shrunk during the deglaciation from the LGM to the present, suggesting that the PV evolved in the same direction as it evolved over the past few decades, despite different mechanisms (Manzini et al., 2012). Therefore, together with previous relevant studies, our results suggest that a warmer climate favors a PV shrinkage and shift towards Eurasia.

Numerous studies of PV variability on inter-annual time scale have suggested that a warming climate with less sea ice in the Barents–Kara Sea region could weaken the PV strength through enhancing the turbulent heat flux (e.g. Kim et al. 2014). Observational analyses have also revealed a "seesaw" pattern in atmospheric mass between the polar cap regions and the surrounding zonal rings under the current warming climate (Kim et al., 2014; Kug et al., 2015). Accordingly, the geopotential height has been found to fall over the polar cap region and to strengthen over the subpolar westerlies from the surface to the lower stratosphere (Thompson et al., 2000). This seems consistent with the overall stronger temporal VSI variability, shown by larger standard deviation, in three LGM simulations than in their PI simulations, with the exception of CESM that has larger temporal variability during PI (that is much larger than observation and other models) than LGM (Fig. S2). This overall enhanced temporal variability is probably related to the ice sheet-related stretching of PV that makes it less stable ellipse shape, which can theoretically increase the possibility of outbreak of cold air. Meanwhile, here we only found a small strengthening of PV during the LGM compared to the PI in some models or even an opposite change in the AWI-ESM, as shown by mean PV strength (Fig. S2). Nevertheless, the LGM response seems compatible with previous climate models results that found that the stratospheric polar vortex itself can be colder or stronger with increasing GHG if the troposphere-originated planetary waves strengthen sufficiently (Baldwin et al., 2003).

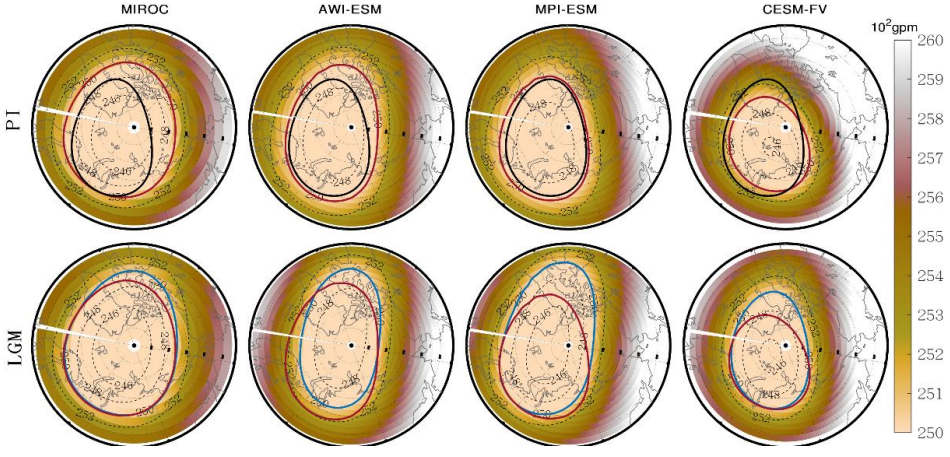

Figure 1 Geopotential height at 20hPa in PI (upper panel) and LGM (lower panel) simulations, illustrating the shape and strength of the Polar Vortex. The dashed contour lines denote $2*10^2$gpm intervals from 246 to $252*10^2$gpm. Black, red and blue lines refer to $250*10^2$gpm for ERA5 re-analysis data (for the period of 1940-2024), PI and LGM, respectively.

https://doi.org/10.5194/cp-2024-46
Preprint. Discussion started: 4 July 2024
© Author(s) 2024. CC BY 4.0 License.

Climate of the Past Discussions

3.2 The impact of polar vortex on mid-latitude climates

3.2.1 Stretched PV enhanced the LGM winter cooling

Compared to the PI, the LGM climate was significantly cooled by the ice sheets, lower GHG, elevated atmospheric dust, and related feedback processes between different components of the climate system. The simulated temperature was cooled by more than 15℃ over the ice sheets. However, a closer look at the temperature changes in the simulations and in proxy-based reconstructions shows a stronger LGM cooling in winter than in summer (Fig. 2). The LGM summer cooling was strictly constrained over the ice sheets, highlighting the controlling effect of ice sheets on summer climate. The primary mechanism of the ice sheets cooling the climate includes elevated altitudes, an enhanced ice-albedo feedback and modified atmospheric circulation (Renssen et al., 2009; Zhang et al., 2016b). By contrast, this enhanced cooling extended further into the mid-latitudes of the continents during the winter. For instance, the -10℃ isotherm line of the LGM winter temperature anomalies extends down south to nearly 30 ℃N in North America that is far beyond the coverage of the Laurentide ice sheet (Fig. 2). This implies that extra processes play a role in cooling the mid-latitudes during winter in addition to the direct ice sheet cooling effects. From the climate forcing perspective, orbital scale insolation could potentially induce seasonal and latitudinal change up to this magnitude. Nevertheless, a very similar LGM orbital setting to the present day (as discussed in Section 2.1) excludes this possibility.

The enhanced LGM cooling over mid-latitudes is probably linked to the stretched polar vortex that is an important driver for mid-latitude climate. First, planetary waves generated by the presence of continental ice sheets could extend the southern boundary of regions where cool air could arrive further south and induce cooling at mid-latitudes (Kolstad et al., 2010). Furthermore, the ellipse shape of PV stretched by the ice sheet can create irregular waves when propagating that is less stable than the round shape PV of the present (Zhang et al., 2022). Both of those factors can lead to an enhanced winter cooling at the mid latitudes during the LGM. The PV-related large variations of winter cooling among these four models contribute to the inter-model spread (will be discussed in Section 3.3.2).

https://doi.org/10.5194/cp-2024-46
Preprint. Discussion started: 4 July 2024
© Author(s) 2024. CC BY 4.0 License.

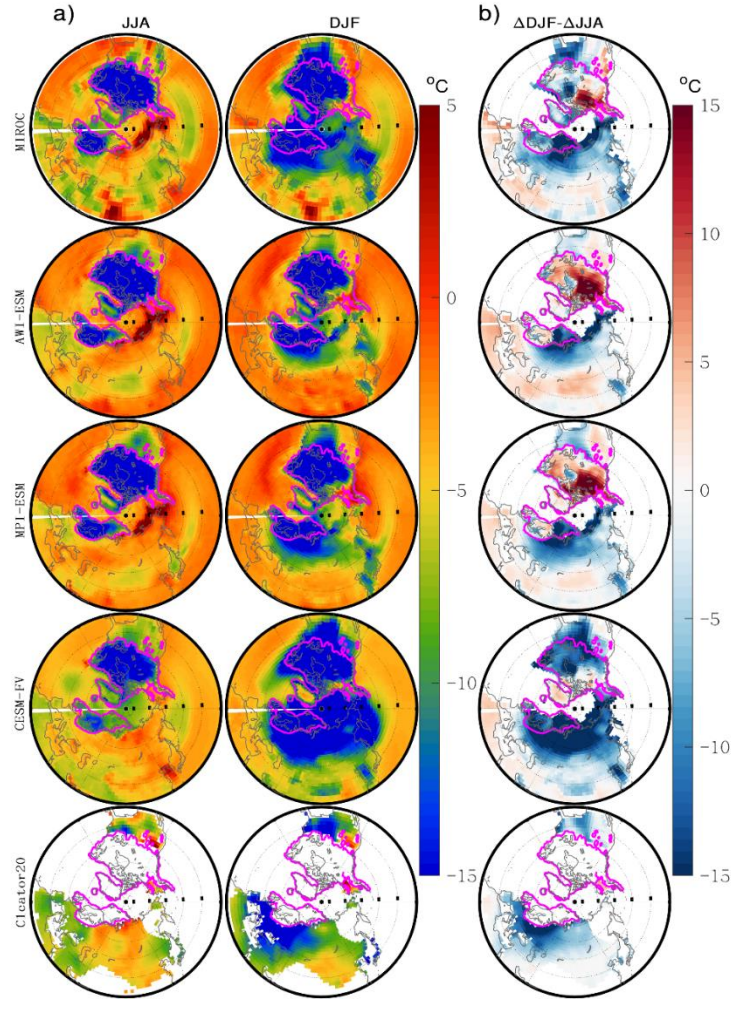

Figure 2 Seasonal LGM temperature anomalies (LGM-PI) (a) and their seasonal differences (b, defined as DJF-JJA from a). The magenta contour line marks the range of ice sheets during LGM.

3.2.2 Linkage of polar vortex variation to winter climate

The composite analysis (i.e. composited winter temperature anomalies) reveals that the effect of a weak PV on climate is shown as a warm-cold-warm-cold pattern on the continent, corresponding to a "dipole pattern" for the Eurasia and N America continents, respectively (Fig. S3). This effect can be further illustrated by the surface air temperature (SAT) difference between the weak and strong PV composite (Fig. 3). The weak PV causes positive temperature differences of ~ 1 ℃ in the south and negative differences up to 2-3℃ in the north with the boundary at 40-45 ℃N over Eurasia. In N America, weak PV causes warm conditions over high latitudes and cold conditions in lower latitudes with a boundary ranging from 45 ℃N in MPI to 30 ℃N in MIROC.

https://doi.org/10.5194/cp-2024-46
Preprint. Discussion started: 4 July 2024
© Author(s) 2024. CC BY 4.0 License.

Climate of the Past Discussions

These patterns can be explained by the atmospheric circulation, as indicated by sea level pressure changes (Fig. 3). A weak PV can result in a weakening of the subpolar low by inducing positive anomalies in sea level pressure and an increase of the subtropical high by prompting negative anomalies over the North Atlantic. This increased polar high facilitates the flow of colder air from the Arctic into Eurasia, while a decreased subpolar low can reduce heat carried by the air from the south. These two processes together cause dipole responses on the Eurasian continent. For the North American continent, the upstream region of the Pacific shows opposite responses and the temperature shows a contrasting dipole pattern (Fig. 3). The results of the winter temperature and surface circulation responses to PV variation fit observational analyses on inter-season and inter-annual variations. The observational analyses have shown a strong connection between the strength of the stratosphere polar vortex and the dominant pattern of surface weather variability, such as the North Atlantic Oscillation (NAO)(Thompson et al., 2000; Yang et al., 2016). In this sense, the slowly varying stratospheric signal may help predict the North Atlantic Oscillation changes and the weather for the coming months (Baldwin and Dunkerton, 2001).

During the LGM, the overall pattern of composite temperature anomalies for weak and strong PSI is similar to the present day (Fig. 3). However, the strength of temperature anomalies is generally enhanced over Eurasia in most of the models, with the exception of CESM. For instance, the cooling anomalies are increased from 2℃ to 3℃ in MIROC. Some other visible differences include the range of warming and cooling. For instance, the negative temperature anomalies over Eurasia extend slightly further south in the LGM than in the PI. Therefore, the difference in surface winter temperature between strong and weak PV conditions during the LGM is up to 2-4℃ in general, which is slightly stronger than PI.

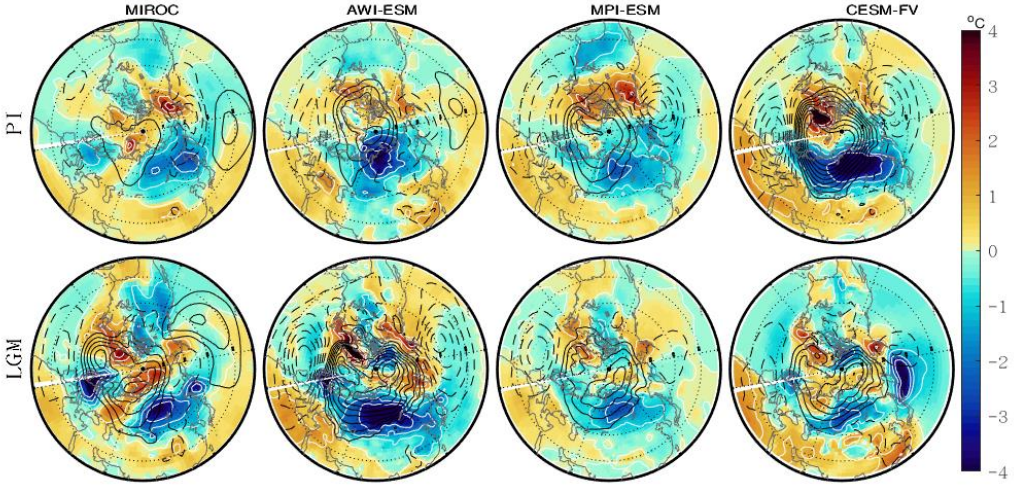

Figure 3 Winter surface air temperature (SAT) differences (filled colour, in ℃) between the weak (low PSI) and strong (high PSI) polar vortex composites for both PI and LGM. The sea level pressure (SLP) (contours, with the interval of 120 hPa) in DJF is also shown.

https://doi.org/10.5194/cp-2024-46
Preprint. Discussion started: 4 July 2024
© Author(s) 2024. CC BY 4.0 License.

Climate of the Past Discussions
Open Access
EGU

3.3 PV variation increases climate variability and uncertainty

3.3.1 Large inter-annual climate variability at mid-latitudes

The spatial distribution of the temperature standard deviation shows large climate variations over mid-latitudinal continents and near the margin of sea ice extension (Fig. 4a). Compared with PI, climate variation during the LGM is overall enhanced over both land and ocean at mid-latitudes. The region of large climate variability moves southward during LGM. This leads to dipole patterns of the temperature variability differences between LGM and PI, with significant enhancement in the south and a reduction in the north (Fig. 4b). The enhanced climate variation over the North Atlantic during the LGM is in line with the southward extended sea ice margin (Fig. 4a & 4b). This implies a controlling role played by dynamic sea ice in climate variability.

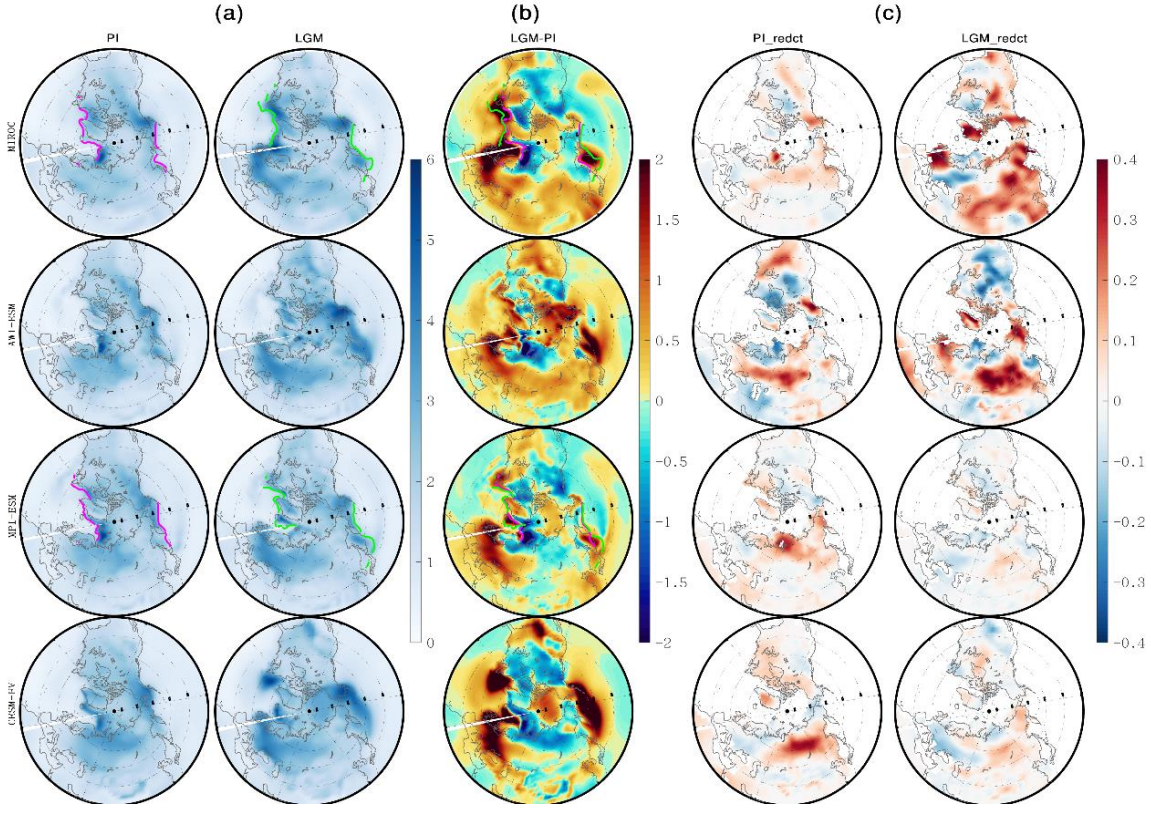

Figure 4 Winter month climate variability, shown as Standard Deviation (SD) of winter temperature for PI and LGM **(a)**, their LGM anomalies **(b**, calculated by (a)-(b)), and the SD reduction **(c)**. The SD reduction is defined as the difference of SD between the total standard deviation and those the strong and weak PV years (i.e. used for the composites) are removed. Magenta and green lines in (a) and (b) indicate the margin of sea ice during winter for the simulations when available (MIROC and MPI-ESM in this case).

https://doi.org/10.5194/cp-2024-46
Preprint. Discussion started: 4 July 2024
© Author(s) 2024. CC BY 4.0 License.

Climate of the Past Discussions

On the land, the enhancement of the LGM climate variability at mid-latitude of Eurasia and North America is visible and probably related to the stretched PV (Fig. 4a & 4b). Removing the strong and weak PV composites can clearly reduce the climate variability over the mid-latitude continents (Fig. 4c). The common feature of this reduction among models is their positive anomalies, despite some variations in their detailed pattern. Compared with PI, the region with the large reduction is located further south during the LGM, which is consistent with a stretched PV. This enhanced climate variability during the winter over the mid-latitudes also appears in previous studies on seasonal climate of LGM (Cleator et al., 2020; Kageyama et al., 2021). The winter temperature variability has been found to be enhanced over the mid- and high-latitudes, which further contributes to a large part of LGM climate variability (Annan et al., 2022; Cleator et al., 2020; Kageyama et al., 2021).

3.3.2 Large inter-model spread of winter temperature

Although the four models give similar patterns of LGM temperature anomalies in general, there are still visible differences. The root mean square deviation of individual models' temperature shows that the winter has a larger inter-model spread than the summer (Fig. 5). The largest inter-model spread was found over the Nordic Seas, which is due to large climate uncertainty induced by dynamic sea ice. Over the continents, the inter-model spread is overall larger than over the oceans, and large values are found over mid-latitudes. This wide mid-latitude spread is the primary contributor to climate uncertainty.

The large spread of multi-models temperatures over the mid-latitudinal continents can be significantly reduced by removing the strong and weak PV composites (Fig.5b). For zonal mean temperature, the winter inter-model spread decreased by almost 0.8℃ for the latitude of 30-50 ℃N when removing the weak and strong PV years. In particular, the reduction over North America is up to 5 ℃, and mainly distributed over 30-45 ℃N (Fig. 5b). For the Eurasian continent, a similar degree reduction is found over the latitude of 40-65 ℃N.

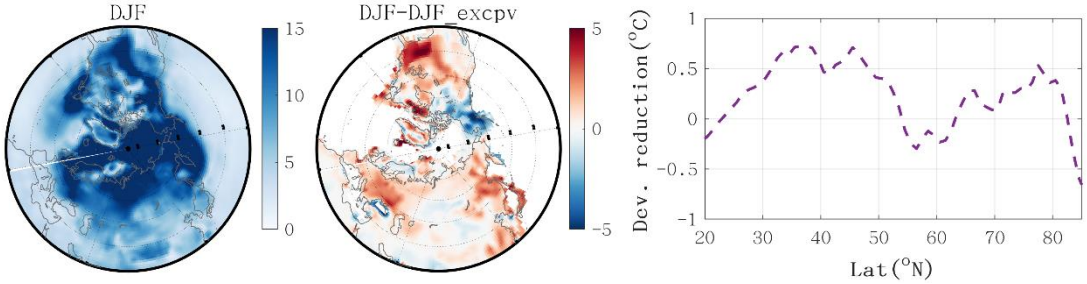

Figure 5 Inter-model spread of LGM temperature anomalies. **(a)** is the inter-model spread of LGM temperature anomalies, defined as the root mean square deviation of LGM anomalies from ensemble mean. **(b)** is the difference between the result in (a) and inter-model spread after remove their weak and strong VSI composites. **(c)** is the latitudinal profile of (b) for the continents.

https://doi.org/10.5194/cp-2024-46
Preprint. Discussion started: 4 July 2024
© Author(s) 2024. CC BY 4.0 License.

Climate of the Past Discussions

Previous studies have found a less consistent winter climate among different models than summer (Harrison et al., 2015; Kageyama et al., 2021). Our analyses identify a previously unknown source for mid-latitudinal climate variability and inter-model spread, suggesting that PV variations need to be taken into account for realistic simulation of climate variability during the glacial-interglacial cycle.

Conclusions

Our analysis of the polar vortex (PV) changes during the LGM suggest that it has a key role in linking the polar and mid-latitudes even in glacial climate and its adaptation according to the glacial-interglacial cycle. PV weakening causes two dipole structures of continental winter temperature for the LGM that are similar to PI, suggesting that the mechanisms of PV affecting the tropospheric climate works for both periods. Comparison of PV between the PI and LGM shows that the during the LGM PV was stretched toward the American continent, which pushes the regions affected by outbreaks of cold air further south. The difference in surface winter temperature between strong and weak PV conditions during the LGM is up to 2-4℃, which is slightly stronger than during the PI. During the LGM, the stretched PV pushed cold Arctic air further equatorward, increasing the mid-latitudinal winter climate variability. Removing the PV variations can reduce inter-annual variability of winter temperature up to 5℃ over mid-latitude Eurasia. PV-induced temperature variability also explains the inter-model spread, as removing PV variation persistently reduces the root mean root mean square deviation mid-latitudes by 0.8℃. These results highlight the critical role of PV in linking the polar and mid-latitudes even in glacial-interglacial timescale.

Competing interests

The contact author has declared that none of the authors has any competing interests.

Acknowledgements

The author would like to acknowledge PMIP4 and specifically to the four involved modelling groups for running the experiments and for making their results available for further analysis.

References

Andrews, D. G., Holton, J. R., and Leovy, C. B., 1987, Middle Atmosphere Dynamics, *in* Andrews, D. G., Holton, J. R., and Leovy, C. B., eds., International Geophysics

https://doi.org/10.5194/cp-2024-46
Preprint. Discussion started: 4 July 2024
© Author(s) 2024. CC BY 4.0 License.

Volume 40, Academic Press, p. 443-462.

Annan, J. D., Hargreaves, J. C., and Mauritsen, T., 2022, A new global surface temperature reconstruction for the Last Glacial Maximum: Climate of the Past, v. 18, no. 8, p. 1883-1896.

Baldwin, M. P., and Dunkerton, T. J., 2001, Stratospheric Harbingers of Anomalous Weather Regimes: Science, v. 294, no. 5542, p. 581-584.

Baldwin, M. P., Thompson, D. W., Shuckburgh, E. F., Norton, W. A., and Gillett, N. P., 2003, Atmospheric science. Weather from the stratosphere?: Science, v. 301, no. 5631, p. 317-319.

Baldwin, M. P., and Thompson, D. W. J., 2009, A critical comparison of stratosphere–troposphere coupling indices: Quarterly Journal of the Royal Meteorological Society, v. 135, no. 644, p. 1661-1672.

Bereiter, B., Eggleston, S., Schmitt, J., Nehrbass-Ahles, C., Stocker, T. F., Fischer, H., Kipfstuhl, S., and Chappellaz, J., 2015, Revision of the EPICA Dome C CO2 record from 800 to 600 kyr before present: Geophysical Research Letters, v. 42, no. 2, p. 542-549.

Braconnot, P., Harrison, S. P., Kageyama, M., Bartlein, P. J., Masson-Delmotte, V., Abe-Ouchi, A., Otto-Bliesner, B., and Zhao, Y., 2012, Evaluation of climate models using palaeoclimatic data: Nature Climate Change, v. 2, no. 6, p. 417-424.

Braconnot, P., and Kageyama, M., 2015, Shortwave forcing and feedbacks in Last Glacial Maximum and Mid-Holocene PMIP3 simulations: Philos Trans A Math Phys Eng Sci, v. 373, no. 2054.

Cai, D., Lohmann, G., Chen, X., and Ionita, M., 2024, The linkage between autumn Barents-Kara sea ice and European cold winter extremes: Frontiers in Climate, v. 6.

Charney, J. G., and Drazin, P. G., 1961, Propagation of planetary-scale disturbances from the lower into the upper atmosphere: Journal of Geophysical Research (1896-1977), v. 66, no. 1, p. 83-109.

Clark, P. U., and Mix, A. C., 2002, Ice sheets and sea level of the Last Glacial Maximum: Quaternary Science Reviews, v. 21, no. 1, p. 1-7.

Cleator, S. F., Harrison, S. P., Nichols, N. K., Prentice, I. C., and Roulstone, I., 2020, A new multivariable benchmark for Last Glacial Maximum climate simulations: Climate of the Past, v. 16, no. 2, p. 699-712.

Danabasoglu, G., Lamarque, J. F., Bacmeister, J., Bailey, D. A., DuVivier, A. K., Edwards, J., Emmons, L. K., Fasullo, J., Garcia, R., Gettelman, A., Hannay, C., Holland, M. M., Large, W. G., Lauritzen, P. H., Lawrence, D. M., Lenaerts, J. T. M., Lindsay, K., Lipscomb, W. H., Mills, M. J., Neale, R., Oleson, K. W., Otto-Bliesner, B., Phillips, A. S., Sacks, W., Tilmes, S., van Kampenhout, L., Vertenstein, M., Bertini, A., Dennis, J., Deser, C., Fischer, C., Fox-Kemper, B., Kay, J. E., Kinnison, D., Kushner, P. J., Larson, V. E., Long, M. C., Mickelson, S., Moore, J. K., Nienhouse, E., Polvani, L., Rasch, P. J., and Strand, W. G., 2020, The Community Earth System Model Version 2 (CESM2): Journal of Advances in Modeling Earth Systems, v. 12, no. 2.

Hajima, T., Watanabe, M., Yamamoto, A., Tatebe, H., Noguchi, M. A., Abe, M., Ohgaito, R., Ito, A., Yamazaki, D., Okajima, H., Ito, A., Takata, K., Ogochi, K., Watanabe, S., and Kawamiya, M., 2020, Development of the MIROC-ES2L Earth system model and the evaluation of biogeochemical processes and feedbacks: Geoscientific Model Development, v. 13, no. 5, p. 2197-2244.

Harrison, S. P., Bartlein, P. J., Izumi, K., Li, G., Annan, J., Hargreaves, J., Braconnot, P., and Kageyama, M., 2015, Evaluation of CMIP5 palaeo-simulations to improve climate projections: Nature Climate Change, v. 5, no. 8, p. 735-743.

Kageyama, M., Albani, S., Braconnot, P et al., 2017, The PMIP4 contribution to CMIP6 – Part 4: Scientific objectives and experimental design of the PMIP4-CMIP6 Last Glacial Maximum experiments and PMIP4 sensitivity experiments: Geoscientific Model Development, v. 10, no. 11, p. 4035-4055.

Kageyama, M., Harrison, S. P., Kapsch, M.-L et al., 2021, The PMIP4 Last Glacial Maximum experiments: preliminary

https://doi.org/10.5194/cp-2024-46
Preprint. Discussion started: 4 July 2024
© Author(s) 2024. CC BY 4.0 License.

results and comparison with the PMIP3 simulations: Climate of the Past, v. 17, no. 3, p. 1065-1089.

Kim, B. M., Son, S. W., Min, S. K., Jeong, J. H., Kim, S. J., Zhang, X., Shim, T., and Yoon, J. H., 2014, Weakening of the stratospheric polar vortex by Arctic sea-ice loss: Nat Commun, v. 5, p. 4646.

Kim, J.-S., Kug, J.-S., Jeong, S., Yoon, J.-H., Zeng, N., Hong, J., Jeong, J.-H., Zhao, Y., Chen, X., Williams, M., Ichii, K., and Schaepman-Strub, G., 2022, Arctic warming-induced cold damage to East Asian terrestrial ecosystems: Communications Earth & Environment, v. 3, no. 1.

Kolstad, E. W., Breiteig, T., and Scaife, A. A., 2010, The association between stratospheric weak polar vortex events and cold air outbreaks in the Northern Hemisphere: Quarterly Journal of the Royal Meteorological Society, v. 136, no. 649, p. 886-893.

Kug, J.-S., Jeong, J.-H., Jang, Y.-S., Kim, B.-M., Folland, C. K., Min, S.-K., and Son, S.-W., 2015, Two distinct influences of Arctic warming on cold winters over North America and East Asia: Nature Geoscience, v. 8, no. 10, p. 759-762.

Manzini, E., Cagnazzo, C., Fogli, P. G., Bellucci, A., and Müller, W. A., 2012, Stratosphere-troposphere coupling at inter-decadal time scales: Implications for the North Atlantic Ocean: Geophysical Research Letters, v. 39, no. 5.

Mauritsen, T., Bader, J., Becker, T et al., 2019, Developments in the MPI-M Earth System Model version 1.2 (MPI-ESM1.2) and Its Response to Increasing CO2: Journal of Advances in Modeling Earth Systems, v. 11, no. 4, p. 998-1038.

McIntyre, M. E., and Palmer, T. N., 1983, Breaking planetary waves in the stratosphere: Nature, v. 305, no. 5935, p. 593-600.

Peltier, W. R., Argus, D. F., and Drummond, R., 2015, Space geodesy constrains ice age terminal deglaciation: The global ICE-6G_C (VM5a) model: Journal of Geophysical Research: Solid Earth, v. 120, no. 1, p. 450-487.

Polvani, L. M., and Waugh, D. W., 2004, Upward Wave Activity Flux as a Precursor to Extreme Stratospheric Events and Subsequent Anomalous Surface Weather Regimes: Journal of Climate, v. 17, no. 18, p. 3548-3554.

Reichler, T., Kim, J., Manzini, E., and Kröger, J., 2012, A stratospheric connection to Atlantic climate variability: Nature Geoscience, v. 5, no. 11, p. 783-787.

Renssen, H., Seppä, H., Heiri, O., Roche, D. M., Goosse, H., and Fichefet, T., 2009, The spatial and temporal complexity of the Holocene thermal maximum: Nature Geoscience, v. 2, no. 6, p. 411-414.

Shi, X., Yang, H., Danek, C., and Lohmann, G., 2020, AWI AWI-ESM1.1LR model output prepared for CMIP6 PMIP midHolocene, Earth System Grid Federation.

Thompson, D. W. J., Wallace, J. M., and Hegerl, G. C., 2000, Annular Modes in the Extratropical Circulation. Part II: Trends %J Journal of Climate, v. 13, no. 5, p. 1018-1036.

Tierney, J. E., Zhu, J., King, J., Malevich, S. B., Hakim, G. J., and Poulsen, C. J., 2020, Glacial cooling and climate sensitivity revisited: Nature, v. 584, no. 7822, p. 569-573.

Yang, X.-Y., Yuan, X., and Ting, M., 2016, Dynamical Link between the Barents–Kara Sea Ice and the Arctic Oscillation: Journal of Climate, v. 29, no. 14, p. 5103-5122.

Zhang, J., Tian, W., Chipperfield, M. P., Xie, F., and Huang, J., 2016a, Persistent shift of the Arctic polar vortex towards the Eurasian continent in recent decades: Nature Climate Change, v. 6, no. 12, p. 1094-1099.

Zhang, M., Yang, X. Y., and Huang, Y., 2022, Impacts of Sudden Stratospheric Warming on Extreme Cold Events in Early 2021: An Ensemble-Based Sensitivity Analysis: Geophysical Research Letters, v. 49, no. 2.

Zhang, Y., Renssen, H., and Seppä, H., 2016b, Effects of melting ice sheets and orbital forcing on the early Holocene warming in the extratropical Northern Hemisphere: Climate of the Past, v. 12, no. 5, p. 1119-1135.

Zhu, J., Otto-Bliesner, B. L., Garcia, R., Brady, E. C., Mills, M., Kinnison, D., and Lamarque, J. F., 2022, Small Impact of

https://doi.org/10.5194/cp-2024-46
Preprint. Discussion started: 4 July 2024
© Author(s) 2024. CC BY 4.0 License.

Stratospheric Dynamics and Chemistry on the Surface Temperature of the Last Glacial Maximum in CESM2(WACCM6ma): Geophysical Research Letters, v. 49, no. 20.